© 1999 Nature America Inc. • http://neurosci.nature.com

The tetrodotoxin-resistant sodium channel SNS has a specialized function in pain pathways

Armen N. Akopian[1], Veronika Souslova[1], Steven England[1,2], Kenji Okuse[1], Nobukuni Ogata[3], Jan Ure[4], Andrew Smith[4], Bradley J. Kerr[5], Steven B. McMahon[5], Sue Boyce[6], Ray Hill[6], Louise C. Stanfa[7], Anthony H. Dickenson[7] and John N. Wood[1]

[1] *Molecular Nociception Group, Department of Biology, Medawar Building, University College, London WC1E 6BT, UK*

[2] *Present address: Pfizer Central Research, Sandwich, Kent, CT13 9NJ, UK*

[3] *Second Department of Physiology, Faculty of Medicine, Hiroshima University, Hiroshima 734, Japan*

[4] *Centre for Genome Research, West Mains Road, Edinburgh EH9 3JQ, UK*

[5] *Department of Physiology, UMDS, St. Thomas Hospital Medical School, Lambeth Road, London SE1 7EH, UK*

[6] *Merck Sharp and Dohme Research Labs, Terlings Park, Harlow, Essex CM20 2QR, UK*

[7] *Department of Pharmacology, University College, London WC1E 6BT, UK*

Correspondence should be addressed to J.N.W. (j.wood@ucl.ac.uk)

Many damage-sensing neurons express tetrodotoxin (TTX)-resistant voltage-gated sodium channels. Here we examined the role of the sensory-neuron-specific (SNS) TTX-resistant sodium channel α subunit in nociception and pain by constructing *sns*-null mutant mice. These mice expressed only TTX-sensitive sodium currents on step depolarizations from normal resting potentials, showing that all slow TTX-resistant currents are encoded by the *sns* gene. Null mutants were viable, fertile and apparently normal, although lowered thresholds of electrical activation of C-fibers and increased current densities of TTX-sensitive channels demonstrated compensatory upregulation of TTX-sensitive currents in sensory neurons. Behavioral studies demonstrated a pronounced analgesia to noxious mechanical stimuli, small deficits in noxious thermoreception and delayed development of inflammatory hyperalgesia. These data show that SNS is involved in pain pathways and suggest that blockade of SNS expression or function may produce analgesia without side effects.

© 1999 Nature America Inc. • http://neurosci.nature.com

Several kinetically and pharmacologically distinct voltage-gated sodium channels are found in dorsal root ganglion (DRG) neurons[1–6]. The TTX-resistant current is insensitive to micromolar concentrations of tetrodotoxin, with a low single-channel conductance, slow activation and inactivation kinetics and a more depolarized activation threshold than other channels[5,6]. At least three types of TTX-resistant sodium currents in DRG have been distinguished electrophysiologically[7,8], and some evidence suggests that these channels are important in the transmission of nociceptive information to the spinal cord. Both bradykinin-dependent release of calcitonin gene-related peptide and the depolarization of dorsal horn neurons elicited through C-fiber activation are insensitive to peripherally applied TTX[9]. In addition, TTX-resistant action potentials have been detected in C-fibers from human sural nerve biopsies[10]. A role for TTX-resistant channels in nociception is supported by the demonstration that some small-diameter sensory neurons (predominantly nociceptors) in culture express only TTX-resistant sodium currents[11].

At least eight sodium channel α subunits occur in DRG that may account for sodium currents detected electrophysiologically[12]. Three TTX-resistant α subunits are known; one channel is expressed selectively in heart muscle[13], whereas SNS (or PN3) is selectively expressed in a subset of small-diameter sensory neurons[14,15]. A transcript encoding a low-threshold, rapidly inactivating, TTX-resistant sodium channel named NaN or SNS-2 has also been identified in sensory neurons[16,17]. To test the hypothesis that TTX-resistant channels have a specialized role in damage sensing, and to examine the role of SNS in nociception, we generated a null-mutant mouse for the TTX-resistant SNS sodium channel. We found that such mice are normal, apart from partial deficits in perception of noxious thermal, mechanical and inflammatory stimuli.

Results

Voltage-gated sodium channel α subunits contain S4-domain voltage sensors that are essential for activity[18,19]. We therefore generated a targeting construct by substituting for exons 4 and 5 of *sns*, which include the S4 voltage sensor of domain I (Fig. 1), a PGK-neo cassette terminating with stop codons in all three frames[20,21]. Mice heterozygous for the targeted allele were intercrossed to derive viable homozygotes that were repeatedly backcrossed onto C57/Bl6 mice to produce congenic lines[22].

The expression of voltage-gated sodium channel α-subunit mRNAs was examined in null mutants. We used northern blots (Fig. 1c) and PCR (Fig. 1d) to examine whether the deletion of functional SNS altered the expression levels of TTX-sensitive α subunits[20]. Both SNS and the TTX-sensitive channel PN-1 are pre-

© 1999 Nature America Inc. • http://neurosci.nature.com

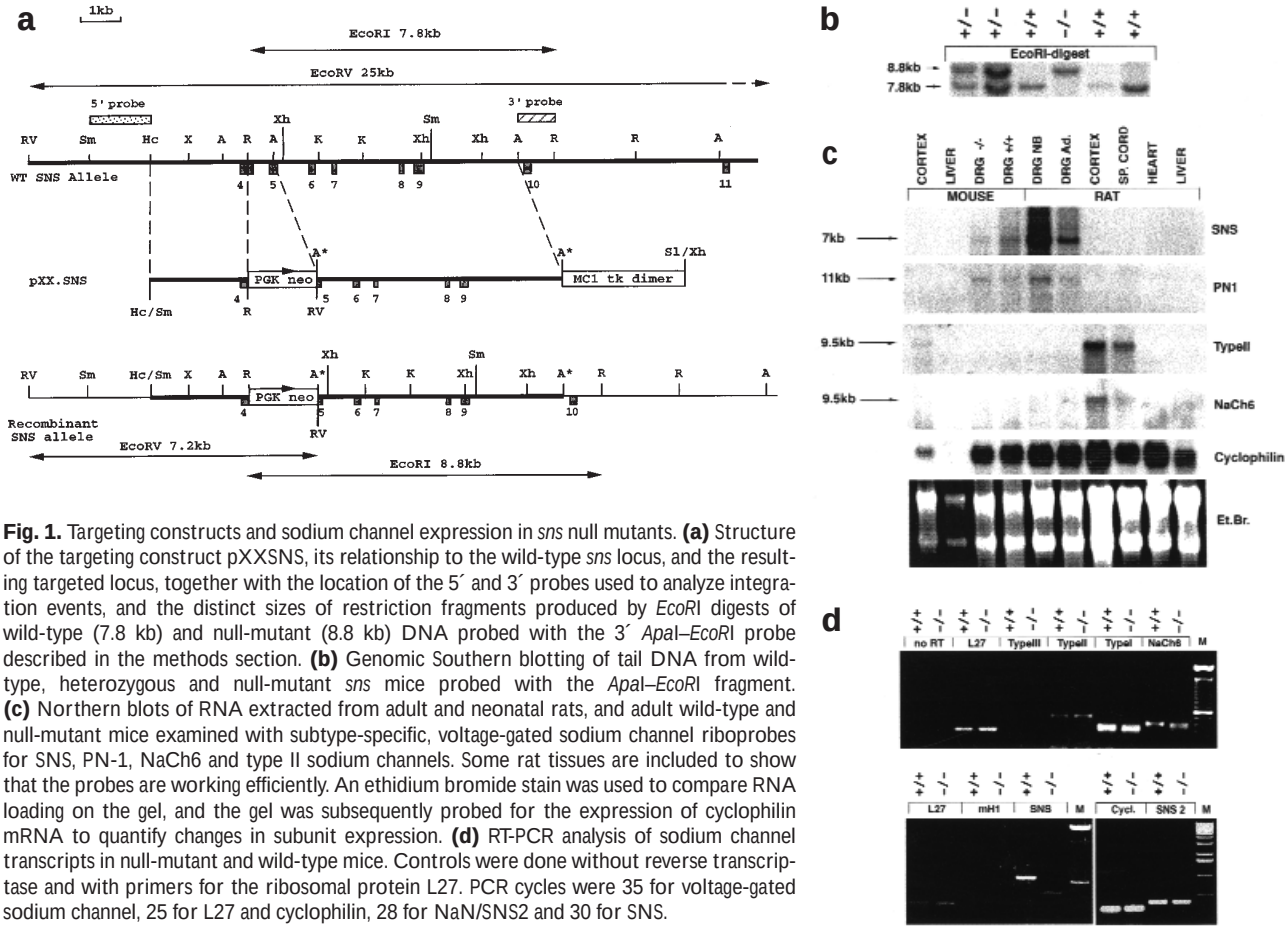

Fig. 1. Targeting constructs and sodium channel expression in *sns* null mutants. **(a)** Structure of the targeting construct pXXSNS, its relationship to the wild-type *sns* locus, and the resulting targeted locus, together with the location of the 5′ and 3′ probes used to analyze integration events, and the distinct sizes of restriction fragments produced by *Eco*RI digests of wild-type (7.8 kb) and null-mutant (8.8 kb) DNA probed with the 3′ *Apa*I–*Eco*RI probe described in the methods section. **(b)** Genomic Southern blotting of tail DNA from wild-type, heterozygous and null-mutant *sns* mice probed with the *Apa*I–*Eco*RI fragment. **(c)** Northern blots of RNA extracted from adult and neonatal rats, and adult wild-type and null-mutant mice examined with subtype-specific, voltage-gated sodium channel riboprobes for SNS, PN-1, NaCh6 and type II sodium channels. Some rat tissues are included to show that the probes are working efficiently. An ethidium bromide stain was used to compare RNA loading on the gel, and the gel was subsequently probed for the expression of cyclophilin mRNA to quantify changes in subunit expression. **(d)** RT-PCR analysis of sodium channel transcripts in null-mutant and wild-type mice. Controls were done without reverse transcriptase and with primers for the ribosomal protein L27. PCR cycles were 35 for voltage-gated sodium channel, 25 for L27 and cyclophilin, 28 for NaN/SNS2 and 30 for SNS.

sent at high levels in peripheral but not central neurons. An SNS transcript running slightly ahead of the wild-type band was detected on northern blots. The levels of PN-1 transcript were upregulated 1.53-fold (s.e. 0.08, $n = 4$, $p < 0.05$) in null-mutant DRG compared to control mice, when transcript levels were normalized against a cyclophilin housekeeping transcript. Using PCR to examine the levels of other less-abundant sodium channel transcripts, we failed to detect the presence of type III or cardiac TTX-resistant transcripts in wild-type or null-mutant DRG. Type-I, NaN/SNS-2, NaCh6 and type II transcripts, in descending order of abundance, were present at roughly equal levels as judged by PCR in wild-type and null-mutant DRG, although up to twofold changes in the levels of transcripts would be difficult to detect reliably using PCR.

Using the same primers for SNS that generated the probes for northern blots, we obtained a weak PCR product representing part of the truncated mRNA from null mutants, whereas a robust signal was apparent in wild-type DRG (Fig. 1d). Sequencing of the null-mutant PCR fragment showed that exons three and six were spliced, causing a frame-shift mutation[20]. Thus a non-functional SNS transcript is made in null mutants, but there is no induction of mRNA encoding TTX-resistant cardiac channel α subunits in these neurons.

Null mutants were healthy, fertile and apparently normal. We examined the sensory neurons in adult L4 DRG by immunocytochemistry. We used antibodies to peripherin to define the small-diameter sensory neurons that express SNS, anti-neurofilament antibody N-52 to define large-diameter, predominantly non-nociceptive, sensory neurons and the lectin IB_4 to stain the *c-ret*-expressing, GDNF (glial cell line-derived neurotrophic factor)-dependent population of sensory neurons[23]. The percentages of stained neurons (41% peripherin positive, 53% N52

Table 1. Distribution of TTX-resistant and TTX-sensitive currents in DRG neurons in culture.

	Wild-type	Heterozygous	SNS null mutant
TTX sensitive			
Current present	30/38 (78.9%)	36/42 (85.7 %)	29/36 (80.6 %)
Current absent	5/38 (13.2%)	3/42 (7.1 %)	2/36 (5.6 %)
Current <0.1 nA	3/38 (7.9%)	3/42 (7.1%)	5/36 (13.9 %)
TTX resistant			
Current present	35/38 (92.1%)	39/42 (92.9 %)	0/36 (0%)
Current absent	3/38 (7.9%)	3/42 (7.1%)	36/36 (100%)
Mean cell capacitance (pF)	24.7 ± 2.6	19.1 ± 1.5	19.7 ± 1.3

Distribution of sodium current types in DRG neurons from wild-type, heterozygous and null-mutant *sns* mice. Mean cell capacitance was not significantly different among the wild-type, heterozygous and null-mutant mice from which cells were prepared.

© 1999 Nature America Inc. • http://neurosci.nature.com

© 1999 Nature America Inc. • http://neurosci.nature.com

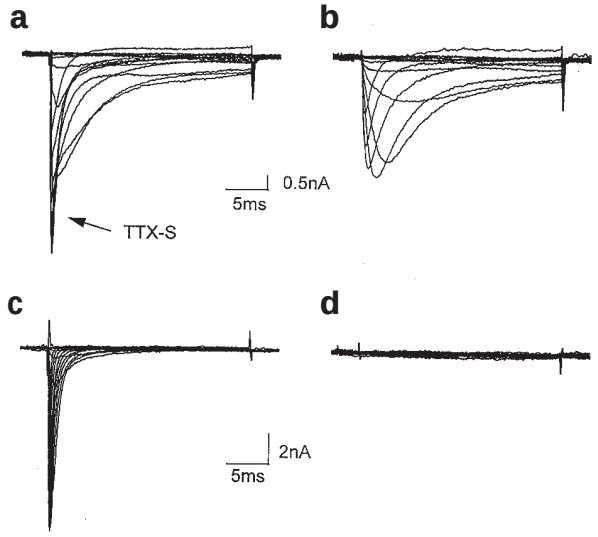

Fig. 2. Functional TTX-resistant sodium channel expression in *sns* null mutants. Sodium currents recorded from wild-type mouse DRG. **(a)** A step to –120 mV in the command potential preceded the step to the test potential. Both fast (TTX-sensitive) and slow (TTX-resistant) currents are apparent. **(b)** Currents recorded from the same cell as **(a)**, but with a prepulse to –50 mV preceding the step to the test pulse. Only the slow TTX-resistant currents are recorded, because of the inactivation of the TTX-sensitive currents. **(c, d)** The same voltage-clamp protocols were used with null-mutant mouse DRG neurons. The currents are rapidly activating and inactivating in **(c)**, whereas with the inactivating prepulse, no current was evoked **(d)**. The recordings were made from small cells of approximately equal size. The capacitances were 16 pF **(a, b)** and 18 pF **(c, d)**.

positive and 28% IB_4 positive) were similar in L4 ganglia of the null-mutant and wild-type mice, as were the total cell numbers determined by counting serial sections through L4 DRG neurons in null mutants (7168 ± 435, n = 3) and wild-type animals (6830 ± 691, n = 3), demonstrating no loss of sensory neurons in the null mutants.

We next examined TTX-sensitive and TTX-resistant voltage-gated sodium currents in wild-type, heterozygous and homozygous null-mutant littermates (Table 1). In wild-type DRG neurons, two types of sodium currents were evoked by step depolarizations (10 ms duration, 5 or 10 mV increments) from a holding potential of –120 mV to between –80 and +40 mV. At low thresholds, this procedure evoked a rapidly activating, rapidly inactivating current, which was sensitive to block by TTX. At higher thresholds, a more slowly activating, slowly inactivating TTX-resistant sodium current became apparent, as observed in mouse C57/Bl6 DRG[24]. We focused on small-diameter neurons (mean capacitance 24 pF) that express most TTX-resistant sodium current[11]. In wild-type DRG neurons (Fig. 2), when a –120 mV prepulse was incorporated into the voltage-clamp protocol, both the fast and slow sodium currents were apparent (Fig. 2a). When a prepulse to –50 mV preceded the change in command potential or cells were treated with 0.5 μM TTX, the TTX-sensitive currents were inactivated, and the slow TTX-resistant currents were recorded in isolation (Fig. 2b). In similar experiments on DRG from null-mutant mice, only the TTX-sensitive current was apparent (Fig. 2c). Injection of null-mutant DRG neurons with a vector encoding the rat α subunit of SNS resulted in the re-expression of large TTX-resistant sodium currents. The characteristics of these exogenously expressed currents (Fig. 3) were indistinguishable from the TTX-resistant currents recorded from DRG neurons from wild-type or heterozygous mice[24]. These experiments confirm that SNS is responsible for all the slow TTX-resistant currents found in sensory neurons. They also demonstrate that there is no requirement for SNS splice variants to rescue the normal TTX-resistant phenotype.

The DRG from wild-type and heterozygous mice showed a mixture of both TTX-sensitive and TTX-resistant sodium currents, whereas a small proportion (8%) of cells in the null mutant expressed neither TTX-sensitive nor TTX-resistant sodium currents. The number of TTX-sensitive cells was similar in DRG from wild-type, heterozygous and null-mutant mice, suggesting that the deletion of *sns* did not alter the cell-type pattern of expression of TTX-sensitive channels. However, when the sodium current densities of DRG neurons from wild-type, heterozygote and null mutants were examined quantitatively, a significant upregulation (about twofold) of TTX-sensitive currents was apparent in null mutants, but not heterozygotes, which were not different from wild-type mice (Fig. 4a).

The significance of altered sodium channel expression was examined by measuring the thresholds of activation of spinal cord wide-dynamic-range neurons by transcutaneous electrical

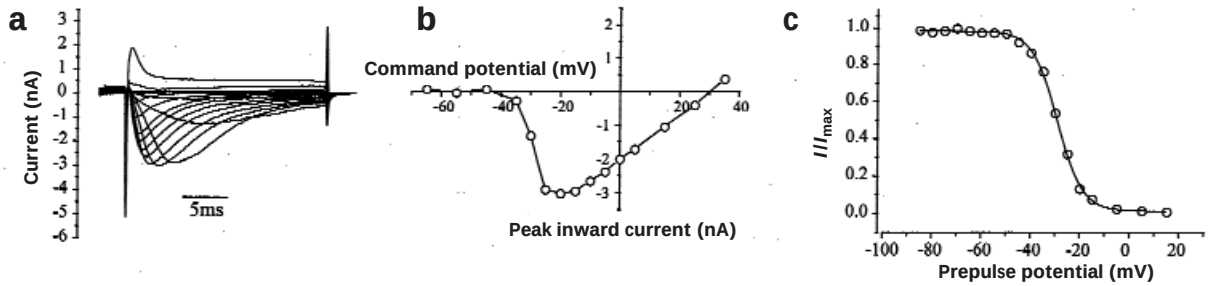

Fig. 3. Rescue of TTX-resistant channels in null mutants following nuclear injection of a vector encoding the α subunit of SNS. The recordings were made in the presence of 500 nM TTX to abolish endogenous TTX-sensitive currents. **(a)** Currents recorded from a null-mutant DRG neuron two days after nuclear injection of the construct. The cell was voltage clamped at –90 mV, prepulsed to –120 mV, and then stepped to a range of potentials (details in text). Slowly activating and inactivating currents were evoked, similar to those in Fig. 2b. **(b)** Current–voltage relationship for the recordings in **(a)**. The threshold for activation of the current was approximately –40 mV, with a peak on stepping to –20 mV. **(c)** Steady-state inactivation curve constructed from currents recorded using the two-pulse protocol detailed in the text. The data has been normalized (I/I_{max}) with respect to current evoked following a non-inactivating prepulse. The data points were fitted by a single Boltzman function, yielding a half-point for inactivation of –29 mV, and a slope factor of 5.1 mV.

© 1999 Nature America Inc. • http://neurosci.nature.com

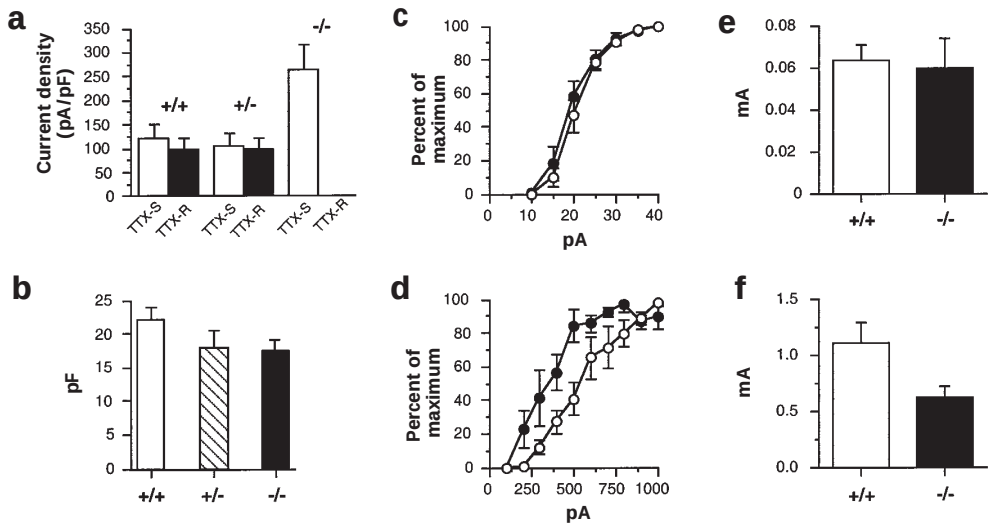

Fig. 4. TTX-sensitive channels are induced in *sns* null mutant C-fiber-associated sensory neurons. **(a)** Whole-cell sodium currents were recorded as indicated in the text. Peak currents were normalized with respect to the capacitances of the individual cells and the data expressed as mean ± s.e.m. ($n > 20$). There was no significant difference between the densities of the tetrodotoxin-sensitive (TTX-S) and tetrodotoxin-resistant currents (TTX-R) in +/+ and +/– mice. In the –/– mice, no TTX-resistant current was detected, whereas the density of TTX-sensitive current was more than twice that found in the two other types of mouse. **(b)** Cell capacitances were measured using the capacitance compensation facility on the amplifier. There was no significant difference in the cell capacitances across the three groups of mice. **(c, d)** Recruitment of A- and C-fibers in the sciatic nerve of wild-type and null-mutant animals. Compound action potentials were recorded from the L4 dorsal roots of urethane-anesthetized animals following electrical stimulation of the sciatic nerve at mid-thigh level. The average compound action potential area is plotted against stimulus strength for A- and C-fibers in **(c)** and **(d)**, respectively (wild type, ○; null mutant, ●; $n = 4$ for both). There is no significant difference in the recruitment curve for A-fibers ($p > 0.05$, Kolmogorov-Smirnov test), but C-fibers in the null mutant animals are activated with significantly less current ($p < 0.01$, Kolmogorov-Smirnov test). **(e, f)** Thresholds of electrical activation of dorsal horn neurons via C-fibers but not A-fibers are lowered in *sns* null mutants. Mean (± s.e.m.) threshold current of transcutaneous electrical stimulation of the hindpaw receptive field required to evoke A-fiber-mediated responses **(e)** or C-fiber-mediated responses **(f)** of dorsal horn neurons recorded in wild-type (+/+; $n = 21$) or null-mutant (–/–; $n = 26$) mice. The C-fiber threshold of electrical excitation **(f)** is lowered in null-mutant mice ($p < 0.05$), whereas A-fiber thresholds **(e)** are identical in the two groups.

© 1999 Nature America Inc. • http://neurosci.nature.com

stimulation. We characterized the responses of 20 wild-type mouse dorsal horn neurons and 26 null-mutant mouse neurons evoked by electrical stimulation of their peripheral receptive fields[25]. In null-mutant mice, the threshold current required to evoke a long-latency (presumably C-fiber mediated) response (Fig. 4f) was significantly lower (0.62 ± 0.09 mA, $n = 26$) than in wild-type mice (1.10 ± 0.19 mA, $n = 20$; Mann-Whitney test, $p = 0.021$). The poststimulus latency of the long-latency evoked response did not differ between the groups (null mutants, 148.5 ± 5.0 ms after stimulus; wild type, 154.9 ± 5.9 ms) suggesting no change in conduction velocity. In contrast, the threshold current required to evoke a short-latency (presumably A-fiber mediated) response (Fig. 4e) was the same in both null-mutant (0.060 ± 0.014 mA) and wild-type mice (0.063 ± 0.008 mA). To confirm that these changes in threshold were due to a lowered threshold for activation of primary afferent C-fibers, recruitment curves were constructed from the areas under the C- and A-fiber waves of compound action potentials recorded from the L4 dorsal roots of wild-type ($n = 4$) and null-mutant mice ($n = 4$). Although no changes were observed in the recruitment of A-fibers (Fig. 4c; $p > 0.05$, Kolmogorov-Smirnov test), C-fibers in the null mutant animals had a lower electrical threshold, and the recruitment curve was shifted significantly to the left (Fig. 4d; $p < 0.01$, Kolmogorov-Smirnov test). With supramaximal electrical stimulation, the latency, waveform and magnitude of A- and C-fiber compound action potentials were similar, suggesting that the differences in recruitment did not result from differences in primary afferent neuron numbers. Consistent with the lowered threshold for evoking a C-fiber latency response in the dorsal horn neurons, the C-fiber recruitment curve in the null mutant animals showed a lowered threshold of activation of these fibers and a significantly higher level of C-fiber activation for a given stimulus intensity than in wild-type mice ($p < 0.01$, Kolmogorov-Smirnov test). The recruitment curves for the acti-

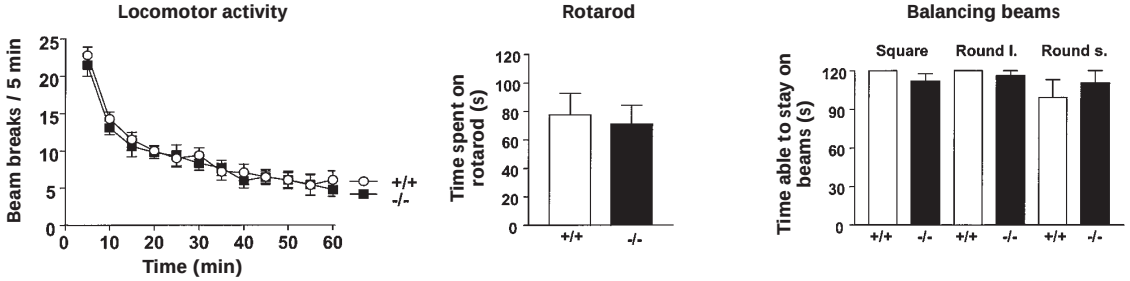

Fig. 5. Normal motor behavior and spinal reflexes in *sns* null mutants. Mice were assessed for sensorimotor coordination using a range of tests. All null mutant and all control mice ($n = 11$) showed normal placing and righting reflexes and hindlimb reflex extension and had no difficulty in maintaining their balance on a beam or on a revolving rotarod. Spontaneous locomotor activity was not different in *sns* mutant and control mice[26].

© 1999 Nature America Inc. • http://neurosci.nature.com

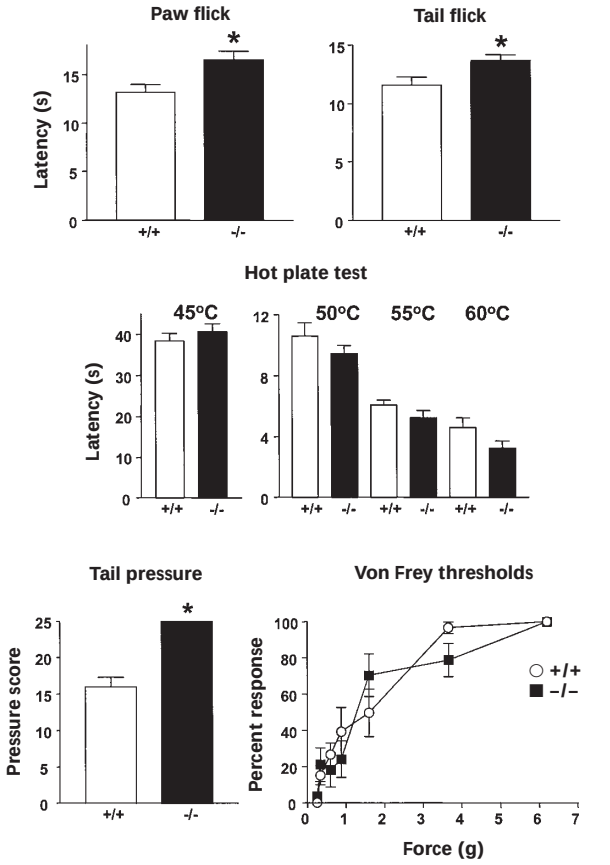

Fig. 6. The *sns* null mutant mice show partial analgesia to noxious thermal and mechanical stimulation. Both paw-flick and tail-flick latencies to noxious irradiation were significantly lengthened in null mutants ($n = 11$, $p > 0.05$), although no differences in hot-plate latencies could be detected at a range of temperatures. Noxious mechanical stimulation provided by Randel-Selitto stimulation showed complete analgesia in null mutant, which all failed to respond up to the cutoff point of the experiment ($n = 11$, $p > 0.005$). In contrast, thresholds to stimulation with Von-Frey hairs were the same in wild-type or null-mutant mice.

vation of A-fibers did not differ between wild-type and null mutant mice ($p > 0.05$, Kolmogorov-Smirnov test). These data (Fig. 4c and d) suggest that the C-fiber-mediated, long-latency input into the dorsal horn of null mutants is more easily stimulated electrically than that of wild-type animals, whereas A-fiber input is identical in wild-type and null-mutant mice. The higher level of expression of TTX-sensitive channels in the somata of DRG null-mutant neurons probably reflects similar altered levels of TTX-sensitive activity in axons and provides a possible mechanism for this alteration in electrical excitability.

Finally, because of the selective expression of SNS in nociceptive sensory neurons, we examined the effect of deleting the SNS channel on mouse behavior, focusing on pain responses. We backcrossed the *sns* null-mutant mice with C57/Bl6 males and found that the behavior of null mutants on different genetic backgrounds from F1 to F4 was identical[22]. Null-mutant mice were indistinguishable in their appearance, spontaneous behavior, body weight and body temperature from age- and sex-matched, wild-type control animals. All null-mutant and wild-type mice exhibited normal placing and righting reflexes and hindlimb reflex extension, and they had no difficulty in maintaining their balance on beams for the full 120-second trial duration (Fig. 5). Similarly, null-mutant mice were able to maintain their balance on a revolving rotorod for the same duration as wild-type mice[26]. Spontaneous locomotor activity was not different in *sns* null-mutant and wild-type mice (Fig. 5).

The responses of null-mutant and wild-type littermates to noxious chemical and thermal stimulation were next examined. The paw-withdrawal and tail-flick latencies following exposure to a noxious thermal (radiant heat) stimulus were significantly increased, albeit to a small extent, in null mutants compared with wild-type mice (Fig. 6). In contrast, there was no difference in the latency on the hot plate of null-mutant and wild-type mice across a range of temperatures (45–60°C; Fig. 6).

Paw-withdrawal responses elicited by graded Von Frey hairs did not differ between null-mutant and wild-type mice (Fig. 6). In contrast, pain thresholds to noxious mechanical stimuli applied to the tail were markedly increased in the null-mutant mice (Fig. 6), which all went to the cutoff point of the test, demonstrating a pronounced mechanical analgesia.

TTX-resistant sodium channels may be involved in persistent inflammatory pain states[27–29]. In wild-type mice, intraplantar injection of carrageenan induced thermal hyperalgesia. Hyperalgesia was apparent at one hour and was maximal for several hours following injection. Thermal hyperalgesia developed more slowly in null-mutant mice, with significant hyperalgesia being observed at two and three hours. However, the maximum level of hyperalgesia was not significantly different in wild-type and null-mutant mice (Fig. 7a and b). Similarly, there was no difference in paw edema in wild-type and null-mutant mice when measured 3.5 hours after the injection of carrageenan (wild-type, 42.1 ± 9.0 mg, $n = 6$; mutant, 37.0 ± 7.7 mg, $n = 6$).

The increased levels of TTX-sensitive currents and lower thresholds of electrical activation of C-fibers could partially compensate for the loss of SNS in null mutants. There are no specific blockers for TTX-sensitive currents, but the local anesthetic lidocaine is a relatively selective blocker of TTX-sensitive currents compared to TTX-resistant sodium currents (IC_{50} of 50 μM for TTX sensitive[4,8,30], 200 μM–1mM for TTX resistant[4,6,31]). Using a systemic dose of lidocaine that had no effect on motor function (25 mg per kg, equivalent to a calculated systemic concentration of approximately 90 μM), we compared the behavior of wild-type and null-mutant littermates. Null-mutant animals showed enhanced thermal hypoalgesia after lidocaine treatment (Fig. 8a; $p < 0.01$, paired t-test), whereas wild-type animals were unaffected ($p > 0.2$, paired t-test). Lidocaine also altered carrageenan-induced hyperalgesia. Three hours after intraplantar carrageenan, when a stable level of hyperalgesia had developed, systemic application of lidocaine produced a partial reversal of the hyperalgesia in wild-type animals, but a complete reversal in null mutants (Fig. 8b; $p < 0.05$, unpaired t-test). These data demonstrate a role for SNS in setting pain thresholds and suggest that TTX-sensitive channel upregulation may compensate for this loss of SNS function in the null mutant.

Discussion

Small-diameter sensory neurons express unusual TTX-resistant sodium channels[1–11], but the absence of subtype-specific sodium channel blockers has precluded a study of the role of individual channel subtypes in nociception. Using gene-targeting technology to delete the TTX-resistant sodium channel *sns*, we find evidence to suggest that there is a selective role for this channel in damage sensing. The normal behavior exhibited by *sns* null

© 1999 Nature America Inc. • http://neurosci.nature.com

© 1999 Nature America Inc. • http://neurosci.nature.com

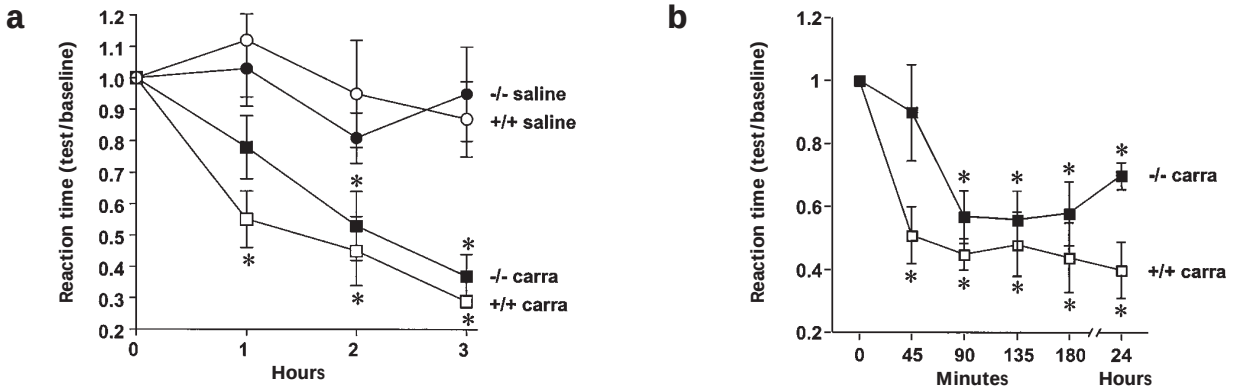

Fig. 7. Full inflammatory hyperalgesia is delayed in the *sns* null mutant. Intraplantar injection of carrageenan induced thermal hyperalgesia at 1 h, and the maximal level of hyperalgesia lasted over 24 h. Thermal hyperalgesia was delayed in null-mutant mice, with significant hyperalgesia ($p > 0.05$) observed only after 90 min. However, the maximum level of hyperalgesia was similar in wild-type and null-mutant mice. Two independent experiments are shown.

© 1999 Nature America Inc. • http://neurosci.nature.com

mutants (apart from deficits in nociception) suggests that SNS is not essential in other aspects of nervous system function, consistent with the highly selective pattern of expression of this channel in sensory neurons[14].

The deletion of *sns* leads to the loss of all slow TTX-resistant currents in sensory neurons clamped at normal resting potentials. However, electrophysiological studies have demonstrated two or more types of TTX-resistant current in DRG neurons[7,8]. These apparently contradictory observations can be reconciled if distinct accessory subunits exist that modify the functional properties of α subunits in a manner analogous to the previously identified sodium channel β subunits[32]. SNS is expressed in two distinct types of sensory neurons, one bearing trkA and p75 and another expressing the GDNF receptor c-ret[23]. It is possible that different cell types express different membrane-associated proteins that influence SNS α-subunit function Alternatively, different TTX-resistant currents may represent distinct phosphorylated states of the same SNS channel[28,29]. These explanations could underlie the observation of type-B and -C TTX-resistant currents[7]. Another TTX-resistant current was observed when small DRG neurons were depolarized from hyperpolarized potentials of –107 mV[7]. The properties of this channel are similar to those recently described for heterologously expressed SNS-2 or NaN[17]. The physiological role of this high threshold current is uncertain, but it will be interesting to analyze the behavioral phenotype of SNS-2/NaN null mutants.

The loss of essentially all TTX-resistant currents in the *sns* null mutant suggests that atypical sodium channels such as NaG[33] are unlikely to encode functional TTX-resistant activity in DRG neurons[17]. Re-injection of constructs encoding SNS into null-mutant DRG neurons reconstituted the repertoire of slow TTX-resistant currents found in normal small-diameter neurons. The *sns* α subunit encodes a channel with aberrant electrophysiological properties when expressed in cell lines or *Xenopus* oocytes[14], raising the possibility that accessory factors that are absent from non-neuronal cells regulate aspects of channel function in DRG neurons.

Concomitant with the loss of SNS, an increased expression of TTX-sensitive currents was observed in the null mutant. The molecular mechanism that links expression of SNS and other sodium channels is unknown[34]. Using the semi-quantitative method of PCR, we could not detect obvious changes in TTX-sensitive α-subunit transcripts. However, northern blots of the abundant PN-1 channel transcript did show an increase in expression of more than 50%. The higher density of TTX-sensitive channels that have a lower threshold of activation than SNS provides an explanation for the diminished threshold of electrical activation of C-fibers but not A-fibers detected both in compound action potential studies of peripheral nerve and in recordings from dorsal horn neurons activated via peripheral stimulation.

Behavioral studies demonstrate a clear-cut deficit in both mechano- and thermoreception and a temporarily diminished response to inflammatory pain stimuli in null-mutant animals backcrossed between one and four times onto a pure C57/Bl6 background. Inflammatory hyperalgesia evoked by prostaglandin E_2 is reversibly blocked by antisense oligonucleotides directed

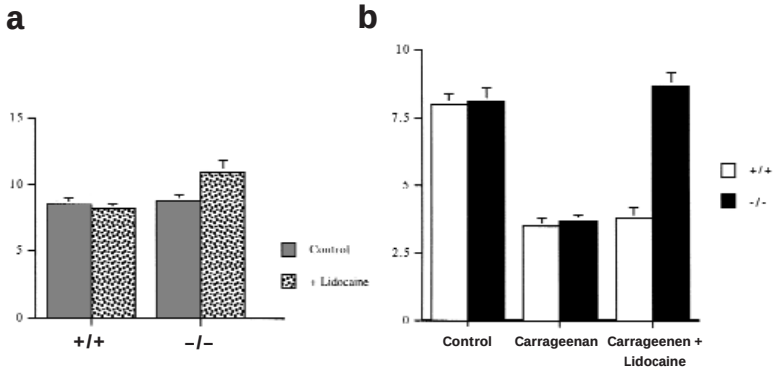

Fig. 8. Systemic lidocaine enhances the analgesic phenotype of *sns* null mutants. **(a)** Baseline thresholds for noxious thermal stimulation with a Hargreaves apparatus were increased in null-mutant animals after lidocaine treatment ($p < 0.01$, paired *t*-test), whereas wild-type animals were unaffected ($p > 0.2$, paired *t*-test). **(b)** Three hours after intraplantar carrageenan injection, both null-mutant (black bars) and wild-type (open bars) animals show a similar level of thermal hyperalgesia. Systemic lidocaine produces a partial reversal of the hyperalgesia in wild-type animals (open bars), but a complete reversal in null mutants (black bars). The responses of null mutants are greater than those of wild-type mice after lidocaine treatment ($p < 0.05$, unpaired *t*-test).

© 1999 Nature America Inc. • http://neurosci.nature.com

against *sns*[39]. The less-pronounced analgesic phenotype demonstrated in null mutants may reflect developmental compensatory mechanisms. Thus the partial analgesia to noxious inflammatory or thermal stimuli could be enhanced by systemic application of lidocaine in the null mutant at doses that do not affect motor behavior, suggesting that the phenotype of the *sns* null mutant would be more pronounced except for the increased expression of TTX-sensitive channels. The delayed development of inflammatory hyperalgesia suggests that targets other than SNS have a later cooperative role in the development of hyperalgesia. Altered potassium current activity is also likely to be involved in setting nociceptor thresholds[38]. The partial analgesia shown by *sns* null mutants is consistent with observations about the role of TTX-resistant currents in nociception[9,10] but is more difficult to reconcile with the expression of higher levels of TTX-sensitive sodium channels and lower electrical activation thresholds of C-fibers in the null mutants. A specialized role for the rapidly repriming TTX-resistant activity encoded by SNS in setting thresholds of depolarization at C-fiber terminals, rather than propagating action potentials, provides a possible explanation for these two sets of observations.

In summary, the data presented here show that the SNS α subunit is responsible for all slow TTX-resistant sodium channel activity in sensory neurons, and that this channel has a selective role in the response of nociceptors to noxious thermal, mechanical and inflammatory stimuli. These observations, combined with other indirect evidence that the regulation of TTX-resistant channels is important in inflammatory pain states[28,29,39] suggest that blockers of SNS synthesis or activity should be specific analgesics.

Methods

Gene targeting. 129Sv genomic DNA was used to construct a targeting vector[20]. A 2.5-kb *Hinc*II–*Eco*RI fragment containing a part of *sns* exon 4 was ligated into pBluescript (linearized with *Sma*I and *Eco*RI) that contained a PGK-neo cassette between the *Eco*RI and *Hind*III sites. An *Apa*I fragment containing exons 5–9 was ligated to the PGK-neo cassette and a thymidine kinase dimer cassette (MC1) to give the targeting construct (Fig. 1a). E14-TG2a subclone IV cells were electroporated with 150 μg *Not*I-linearized vector in 600 μl PBS at 0.8 kV, 3.0 mF. Cells were selected with GM418 and gancyclovir, and three correctly targeted single-copy integrations were identified. Clones were injected into C57BL/6 blastocysts subsequently implanted into CBA × C57BL/6 F1 foster mothers. Male chimeras when crossed with C57BL/6 females gave 100% germline transmission of ES cell coat color. Transmission of the targeted allele was confirmed by Southern blot analysis (Fig. 1a). Chimeras were also subsequently crossed with 129/Sv females. Digests of tail DNA with *Eco*RI were Southern blotted and probed with a random-prime-labeled *Apa*I–*Eco*RI genomic fragment[20] (Fig. 1a). Null-mutant digests containing the PGK-neo cassette produce a band of 8.8 kb, compared to the 7.8-kb band found in wild-type animals (Fig. 1b).

Sodium channels in null-mutant DRG. Probes for sodium channels were cloned by PCR, or the same primers were used in RT-PCR experiments: SNS, X92184, 5′-CAGAGATCGAGAAGCAGATCGCTG-3′, 5′- AGCTTCCTCACTGAGTGGATC-3′; NaN, AF059030, 5′-CCCTGCTGCGCTCGGTGAAGAA-3′, 5′-GACAAAGTAGATCCCAGAGAGG-3′; NaCh6, U59966, 5′-GAGAATGAGTTCGCAGACGATG-3′, 5′-CTCTTCCAGCTCTTCACTAGCGTG-3′; PN-1, X82835, 5′-AGTGCAGTGGACTGCAATGGAGTCG-3′, 5′-GAGCAAATCTGTACCACCATGGTGGACA-3′; Type I, X03638, 5′-GGGAAGATGCACAGCACAGTGGATTCC-3′, 5′-CTTTTAGCCAATATGGAGAACAG-3′; Type II, X03639, 5′-CCGAAAATGACTTTGCAGACGATG-3′, 5′-CCATCACTACCAGATTGACAACGTG-3′; Type III, Y00766, 5′-AAGTCGGAATCGGAAGACAGTGT-3′, 5′-AGGATACTGGCTATGCTCATGGATC-3′; mH1, A33996, 5′-TGAGGCGGACTTCGCAGATGACGAG-3′; 5′-GAGGACACTGACAGCGCTGAGTGCCCG-3′; L-27, 5′-ATCGCTCCTCAAACTTGACC-3′, 5′-AAAGCCGTCATCGTAAAGAAC-3′; cyclophilin 5′- ACCCCACCGTGTTCTTCGAC-3′, 5′- CATTTGCCATGGACAAGATG-3′. Random-primed cDNA synthesized from DNase-I-treated RNA was amplified (94ºC, 1 min), annealed (58ºC, 1 min) and extended (72ºC, 1 min) for 25, 30 or 35 cycles. Amplified DNA was sequenced. [α-^{32}P]UTP-labeled riboprobes were generated from the linearized plasmid using Sp6 or T7 polymerase. We separated 10–30 μg total RNA from rat and mouse tissues on 1% agarose-formaldehyde gels and blotted it onto Hybond-N. Northern blots were done and quantified as described[33]. Bands were normalized against cyclophilin.

Immunocytochemistry. Seven-micron sections of paraformaldehyde-fixed L4 DRG were stained with antibodies against peripherin, and neurofilaments (N52) and with the FITC-labelled lectin IB_4. Strongly positive cell percentages were estimated by counting the total number of neurons. Total cell counts were done by counting nuclei in serial sections of L-4 DRG as described[36].

Electrophysiology. We recorded from DRG neurons (1–5 days in culture) two hours after replating at room temperature. The cDNA encoding rat SNS in the expression vector pGW-1 (*Hind*III–*Kpn*I[35]; 200 μg/ml), together with the GFP expression vector pGW-1-GFP (100 μg/ml) and 0.5 % FITC-dextran were injected into neuronal nuclei. The DNA injection buffer contained 118 mM NaCl, 3 mM KCl, 5 mM HEPES, 22.2 mM $NaHCO_3$ and 1.2 mM $MgCl_2$, pH 7. Recordings were made 1–2 days after injection using the whole-cell, patch-clamp technique[36]. pClamp6 software (Axon) was used to acquire and analyze the currents. Pipets had DC resistances of 3 MΩ. The pipet solution contained 130 mM CsCl, 10 mM NaCl, 1 mM $MgCl_2$, 10 mM HEPES and 5 mM EGTA, pH 7.35. In some experiments, CsCl was substituted with equimolar CsF. The extracellular solution contained 105 mM choline Cl, 35 mM NaCl, 3 mM CsCl, 1 mM $MgCl_2$, 0.01 mM $CaCl_2$, 0.05 mM $CdCl_2$, 11 mM glucose and 5 mM HEPES, pH 7.4. In some experiments, 500 nM TTX was included in the extracellular solution. The extracellular sodium concentration was lowered to 35 mM to reduce the magnitude of the currents. Calcium channel activity was blocked by the inclusion of either CsF in the intracellular or $CdCl_2$ in the extracellular solution.

For electrophysiological studies *in vivo*, mice were anesthetized with urethane (3 g per kg, i.p.) Following a laminectomy, single-neuron extracellular recordings were made using a parylene-coated tungsten electrode in the dorsal horn (120–780 μm; mean depth, 445 ± 28 μm). Electrical stimulation (2 ms pulse) in the peripheral receptive field evoked a short-latency, low-threshold response (< 10 ms after stimulus) and a longer-latency, high-threshold response (100–200 ms after stimulus) in the dorsal horn neuron, which reflect recruitment of A- and C-fibers. Electrical excitability was measured directly by studying compound action potentials from L4 dorsal roots of mice (n = 4) following electrical stimulation of the sciatic nerve at mid-thigh level. Compound action potential areas were measured after square-wave current pulses of 200 μs duration and 0–40 μA amplitude for A-fibers, and 2 ms duration and 0–1 mA amplitude for C-fibers.

Behavioral studies. Mice were examined for spinal reflexes and motor skills as described in detail elsewhere[26]. Nociceptive thresholds to thermal stimuli were determined using hot-plate (45, 50, 55 or 60ºC), paw-flick (method of Hargreaves) or tail-flick methods. For the hot plate, the latency for the mouse to lick its hindpaw or jump was recorded. Paw-flick latencies were determined for both hind paws on three occasions. Tail-flick latencies were determined on three occasions. Mechanical sensitivity was determined using calibrated Von Frey hairs. Hairs were applied three times each in ascending order of force, through a mesh floor, until a response was elicited (paw withdrawal, shaking or biting). Percent responses were calculated for each hair. Nociceptive thresholds to noxious mechanical stimuli were determined using a Ugo Basile algesiometer. The tail was gradually compressed until an escape response was elicited (biting the apparatus, vocalization or struggle). Carrageenan-induced thermal hyperalgesia was assessed[27] using an intraplantar injection of 20 μl of carrageenan (0.6 mg) or saline into one hind paw. Paw-flick

© 1999 Nature America Inc. • http://neurosci.nature.com

© 1999 Nature America Inc. • http://neurosci.nature.com

latencies were measured, and mice that had received carrageenan were killed and both hind feet weighed to measure edema. To assess the effect of lidocaine, after baseline thermal and mechanical measurements, 25 mg per kg lidocaine (Sigma) in PBS (5 mg/ml) was injected i.p. and further tests carried out ten minutes later.

These experiments were carried out under Home Office supervision at UMDS and MSD laboratories.

Acknowledgements

This work was supported by the MRC (V.S., K.O., B.K., S.M., A.H.D., L.C.S.), the Wellcome Trust (A.A., S.E., J.N.W.) and the Royal Society (N.O.). L.C.S. was supported by a Merck Pharmacology Fellowship. The Centre for Genome Research was supported by the BBSRC. We are grateful to Samantha Ravenall, Madhu Sukumaran, Oro Rufian, Stuart Stevenson, Richard Pugh, Jane Haley, Patrique Delmas and David Brown for technical advice and comments.

Received 13 November 1998; accepted 16 April 1999

1. Matsuda, Y., Yoshida, S. & Yonezawa, T. Tetrodotoxin sensitivity and Ca^{2+} component of action potentials of mouse dorsal root ganglion cells cultured in vitro. *Brain Res.* 154, 69–82 (1978).
2. Fukuda, J. & Kameyama, M. TTX-sensitive and TTX-resistant sodium channels in tissue cultured spinal ganglion neurons from adult mammals. *Brain Res.* 182, 191–197 (1980).
3. Rizzo, M. A. Kocsis, J. D. & Waxman, S. G. Slow sodium conductances of dorsal root ganglion neurons: intraneuronal homogeneity and interneuronal heterogeneity. *J. Neurophysiol.* 72, 2796–2815 (1994).
4. Ogata, N. & Tatebayashi, H. Kinetic analysis of two types of sodium channels in rat dorsal root ganglia. *J. Physiol. (Lond.)* 466, 9–37 (1993).
5. Elliott, A. A. & Elliott, J. R. Characterization of TTX-sensitive and TTX-resistant sodium currents in small cells from adult rat dorsal root ganglia. *J. Physiol. (Lond.)* 463, 39–56 (1993).
6. Roy, M. L. & Narahashi, T. Differential properties of TTX-sensitive and TTX-resistant sodium currents in rat dorsal root ganglion neurons *J. Neurosci.* 12, 2104–2111 (1992).
7. Rush, A. M., Brau, M. E., Elliott, A. A. & Elliott, J. R. Electrophysiological properties of sodium current subtypes in small cells from adult rat dorsal root ganglia. *J. Physiol. (Lond.)* 511, 771–789 (1998).
8. Scholz, A., Appel, N. & Vogel, W. Two types of TTX-resistant and one TTX-sensitive Na^+ channel in rat dorsal root ganglion neurons and their blockade by halothane. *Eur. J. Neurosci. Suppl.* 10, 2547–2556 (1998).
9. Jeftinija, S. Bradykinin excites tetrodotoxin-resistant primary afferent fibres. *Brain Res.* 665, 69–76 (1994).
10. Quasthoff, S., Grosskreutz, J., Schroder, J. M., Schneider, U. & Grafe, P. Calcium potentials and tetrodotoxin-resistant sodium potentials in unmyelinated C fibres of biopsied human sural nerve. *Neuroscience* 69, 955–965 (1995).
11. Ogata, N. & Tatebayashi, H. Ontogenic development of the TTX-sensitive and TTX-insensitive Na^+ channels in neurons of the rat dorsal root ganglia. *Brain Res. Dev. Brain Res.* 65, 93–100 (1992).
12. Okuse, K., Akopian, A. N., Sivilotti, L., Dolphin, A. C. & Wood, J. N. in *Molecular Basis of Nociception* (ed. Borsook, D.) 239–257 (IASP, Seattle, 1997).
13. Rogart, R. B., Cribbs, L. L., Muglia, L. K., Kephart, D. D. & Kaiser, M. W. Molecular cloning of a putative tetrodotoxin-resistant rat heart Na^+ channel isoform. *Proc. Natl. Acad. Sci. USA* 20, 8170–8174 (1989).
14. Akopian, A. N., Sivilotti, L. & Wood, J. N. A tetrodotoxin-resistant sodium channel expressed by C-fibre-associated sensory neurons. *Nature* 379, 257–262 (1996).
15. Sangameswaran, L. *et al.* Structure and function of a novel voltage-gated TTX-resistant sodium channel specific to sensory neurons. *J. Biol. Chem.* 271, 5953–5956 (1996).
16. Dib-Hajj, S. D., Tyrrell, L., Black, J. A. & Waxman, S. G. NaN, a novel voltage-gated Na channel, is expressed preferentially in peripheral sensory neurons and down-regulated after axotomy. *Proc. Natl. Acad. Sci. USA* 95, 8963–8968 (1998).
17. Tate, S. *et al.* Two sodium channels contribute to the TTX-R sodium current in primary sensory neurons. *Nat. Neurosci.* 1, 653–655 (1998).
18. Stuhmer, W. *et al.* Structural parts involved in activation and inactivation of the sodium channel. *Nature* 339, 597–603 (1989).
19. Yang, N., George, A. L. & Horn, R. Molecular basis of charge movement in voltage-gated sodium channels. *Neuron* 16, 113–122 (1996).
20. Souslova, V. A., Fox, M., Wood, J. N. & Akopian, A. N. Cloning and characterization of a mouse sensory neuron tetrodotoxin-resistant voltage-gated sodium channel gene, Scn9a. *Genomics* 41, 201–209 (1997).
21. Mansour, S. L, Thomas, K. R. & Capecchi, M. R. Disruption of the proto-oncogene int-2 in mouse embryo-derived stem cells: a general strategy for targeting mutations to non-selectable genes. *Nature* 336, 348–352 (1988).
22. Gerlai, R. Gene-targeting studies of mammalian behavior: is it the mutation or the background genotype? *Trends Neurosci.* 19, 177–181 (1996).
23. Bennett, D. L. *et al.* A distinct subgroup of small DRG cells express GDNF receptor components and GDNF is protective for these neurons after nerve injury. *J. Neurosci.* 18, 3059–3072 (1998).
24. Pearce, R. J. & Duchen, M. R. Differential expression of membrane currents in dissociated mouse primary sensory neurones. *Neuroscience* 63, 1041–1056 (1994).
25. Stanfa, L. C., Misra, C. & Dickenson, A. H. Amplification of spinal nociceptive transmission depends on the generation of nitric oxide in normal and carrageenan rats. *Brain Res.* 737, 92–98 (1996).
26. Boyce, S. *et al.* Onset and progression of motor deficits in motor neuron degeneration (Mnd) mice are unaltered by the glycine/NMDA receptor antagonist L-701,324 or the MAO-B inhibitor R(-)-deprenyl. *Exp. Neurol.* 155, 49–58 (1999).
27. Rupniak, N. M. *et al.* Effects of the bradykinin B1 receptor antagonist des-Arg9[Leu8]bradykinin and the genetic disruption of the B2 receptor on nociception in rats and mice. *Pain*, 71, 89–97 (1997).
28. Gold, M. S., Reichling, D. B., Shuster, M. J. & Levine, J. D. Hyperalgesic agents increase a tetrodotoxin-resistant Na^+ curent in nociceptors. *Proc. Natl. Acad. Sci.USA* 93, 1108–1112 (1996).
29. England, S., Bevan, S. & Docherty, R. J. PGE2 modulates the tetrodotoxin-resistant sodium current in neonatal rat DRG neurones via the cAMP-protein kinase A cascade. *J. Physiol. (Lond.)* 495, 429–440 (1996).
30. Scholz, A., Kuboyama, N., Hempelmann, G. & Vogel, W. Complex blockade of TTX-resistant Na^+ currents by lidocaine and bupivacaine reduce firing frequency in DRG neurons. *J. Neurophysiol.* 79, 1746–1754 (1998).
31. Brau, M. E. & Elliott, J. R. Local anaesthetic effects on TTX-r sodium currents in rat dorsal root ganglion neurones *Eur. J. Anaesthesiol.* 15, 80–88 (1998).
32. Isom, L. L., De-Jongh, K. S. & Catterall, W. A. Auxiliary subunits of voltage-gated ion channels. *Neuron* 12, 1183–1194 (1994).
33. Akopian, A. N., Souslova, V., Sivilotti, L. & Wood, J. N. Structure and distribution of a broadly expressed atypical sodium channel. *FEBS Lett.* 400, 183–187 (1997).
34. Cummins, T. R. & Waxman, S. G. Downregulation of tetrodotoxin-resistant sodium currents and upregulation of a rapidly repriming tetrodotoxin-sensitive sodium current in small spinal sensory neurons after nerve injury. *J. Neurosci.* 17, 3503–3514 (1997).
35. Connolly, C. N., Krishek, B. J., McDonald, B. J., Smart, T. G. & Moss, S. J. Assembly and cell surface expression of heteromeric and homomeric gamma-aminobutyric acid type A receptors. *J. Biol. Chem.* 271, 89–96 (1996).
36. Hamill, O. P., Marty, A., Neher, E., Sakmann, B. & Sigworth, F. J. Improved patch-clamp techniques for high resolution curent recording from cells and cell-free membrane patches. *Pflugers Arch.* 391, 85–100 (1981).
37. Wright, D. E., Zhou, L., Kucera, J. & Snider, W. D. Introduction of a NT-3 transgene into muscle selectively rescues proprioreceptive neurons in mice lacking endogenous NT-3. *Neuron* 19, 503–517 (1997).
38. Gold, M. S, Shuster, M. J. & Levine, J. D. Characterization of six voltage-gated K+ currents in adult rat sensory neurons. *J. Neurophysiol.* 75, 2629–2646 (1996).
39. Khasar, S. G., Gold, M. S. & Levine, J. D. A tetrodotoxin-resistant sodium current mediates inflammatory pain in the rat. *Neurosci. Lett.* 256, 17–20 (1998).

© 1999 Nature America Inc. • http://neurosci.nature.com